

32ND INTERNATIONAL COSMIC RAY CONFERENCE, BEIJING 2011



Microwave detection of cosmic ray showers at the Pierre Auger Observatory

PATRICK S. ALLISON¹, FOR THE PIERRE AUGER COLLABORATION²

¹*Ohio State University, Columbus, OH 43210, United States*

²*Observatorio Pierre Auger, Av. San Martín Norte 304, 5613 Malargüe, Argentina*

(Full author list: http://www.auger.org/archive/authors_2011_05.html)

auger_spokespersons@fnal.gov

Abstract: Microwave emission from the electromagnetic cascade induced in the atmosphere by ultra-high energy cosmic rays (UHECR) may allow for a novel detection technique, which combines the advantages of the well-established fluorescence technique - the reconstruction of the shower profile - with a 100% duty cycle, minimal atmospheric attenuation and the use of low-cost commercial equipment. Two complementary techniques are currently being pursued at the Pierre Auger Observatory. AMBER (Air-shower Microwave Bremsstrahlung Experimental Radiometer), MIDAS (Microwave Detection of Air Showers) and FDWave are prototypes for a large imaging dish antenna. In EASIER (Extensive Air Shower Identification using Electron Radiometer), the microwave emission is detected by antenna horns located on each surface detector of the Auger Observatory. MIDAS is a self-triggering system while AMBER, FDWave, and EASIER use the trigger from the Auger detectors to record the emission. The coincident detection of UHECR by the microwave prototype detectors and the fluorescence and surface detectors will prove the viability of this novel technique. The status of microwave R&D activities at the Pierre Auger Observatory will be reported.

Keywords: Pierre Auger Observatory, microwave, radio, detectors

1 Introduction

The observation of microwave emission from electromagnetic cascades at accelerator experiments in 2003 and 2004, along with results from a simple prototype detector [1] suggest that the ultra-high energy cosmic rays (UHECRs) may be detectable from microwave emission alone. Since microwave attenuation in the atmosphere is minimal (less than 0.05 dB km^{-1} [2]) and the noise temperature of the sky is relatively small (below 10 K for zenith angles less than 60°), a UHECR microwave detector could benefit from the longitudinal observation of the air shower profile with 100% duty cycle and minimal atmospheric loss concerns.

To demonstrate whether or not microwave detection is feasible, several detectors have been developed to operate in conjunction with the Pierre Auger Observatory.

2 AMBER

The AMBER detector is an upgrade from the Gorham et al. prototype [1], consisting of a 2.4 m low-emissivity off-axis parabolic dish with a look angle of 30 degrees, viewed by 4 dual-polarization, dual-band (C: 3.4–4.2 GHz and Ku: 10.95–14.5 GHz) and 12 single-polarization C-band antenna horns. The signal from the antenna horns is passed through a low-noise block (LNB) which ampli-



Figure 1: The upgraded AMBER antenna array installed at the HEAT enclosure at the Pierre Auger Observatory.

fies and downconverts the signal to below 2 GHz, where it is put into a logarithmic (progressive-compression) power detector which produces a signal roughly proportional to the observed radio frequency (RF) power (in dBm). The installed AMBER detector is shown in Fig. 1.

The goal of the upgraded AMBER detector is to observe cosmic ray showers in coincidence with surface detectors of the Pierre Auger Observatory without self-triggering. The Surface Detector (SD) trigger latency is very long - nominally 5 s, however, a modified array trigger (T3) algorithm was developed which outputs approximately 70%

of all T3s within 3 s. The signals from the power detector are digitized at 100 MHz and placed into a large circular buffer (32 GB for all input channels). Time within the circular buffer is tracked using a GPS pulse-per-second (PPS) output and a 100 MHz clock for in-second tracking. The accuracy of this procedure was measured by placing the GPS PPS signal into one input channel, and requesting data around the second boundary. From this, an observed time resolution of 11 ns was obtained.

When the SD registers a possible cosmic ray via a T3 trigger, an approximate time at ground, core location, and incident direction will be derived from the trigger times and tank positions. From the time, location, and direction provided from this reconstruction, the time that the shower crosses the AMBER field of view (FOV), if at all, is then calculated, and the data corresponding to that time will be read out. From a comparison with fully-reconstructed Auger events, the approximation is valid to within 10° degrees in solid angle and 500 m in core position. For all cosmic rays within the AMBER FOV, this accuracy is sufficient for a reasonable readout window (100 μ s) to contain a possible cosmic ray track.

The calibration of the AMBER instrument was done by first injecting a signal of varying power from a network analyzer into the power detector modules to convert the signal seen at the digitizer to power observed at the power detector input. Next, the front of the feed array was placed into a liquid nitrogen bath in an anechoic chamber to perform a Y-factor measurement to calibrate the gain and noise figure of the LNB to obtain the power at the input of the feed array. Finally, the dish itself was calibrated separately using a Y-factor measurement using RF absorber foam and a calibrated LNB. The combined system noise temperature ranges from ~ 45 K for the outer single-band antennas, and ~ 65 K for the inner antennas in C-band. Ku-band system temperatures were significantly higher (~ 100 K) due to the LNBs.

The upgraded AMBER system was in operation at the University of Hawaii from January to June 2010. A search for cosmic ray candidates was performed using a separate self-trigger board. However, the RF environment was significantly worse than during the operation of the original prototype, and no candidates were found. During the operation period, several observations of Sun transits were performed to validate the expected optical performance, as seen in Fig. 2. The full-width at half-max (FWHM) of the Sun was 2.4° , and the expected FWHM based on the dish characteristics was 2.3° , giving a total field of view of $\approx 7^\circ \times 7^\circ$.

Following the operation in 2010, the AMBER detector was packaged and shipped to Argentina. The detector was re-assembled and integrated at the Coihueco Fluorescence Detector (FD) site, alongside the HEAT [3] fluorescence telescopes (which have a similar viewing angle), and overlooking the SD infill array. Data taking in coincidence with the Auger SD is currently underway.

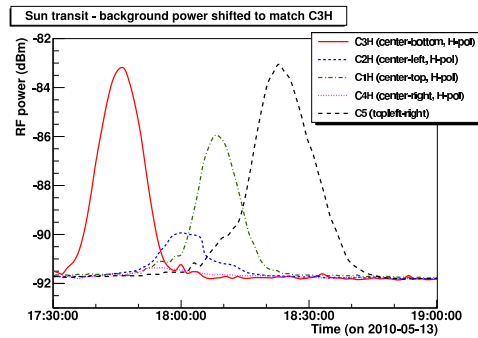


Figure 2: RF power as a function of time for a Sun transit observed by AMBER. The Sun’s path was directly through the C3H/C5 pixels, partially through the C1H/C2H pixels, and not directly in C4H at all. Observed FWHM for the Sun was 2.4° , compared to an expected 2.3° for the dish geometry.



Figure 3: The MIDAS prototype at the University of Chicago.

3 MIDAS

The MIDAS detector (shown in Fig. 3) consists of a 4.5 m parabolic reflector with a 53-pixel camera with 7 rows of 7 or 8 pixels, arranged in a staggered layout to maximize coverage. The pixel’s field of view ($\approx 1.3^\circ \times 1.3^\circ$ at center) depends on its position on the camera due to aberrations, for a total camera FOV of $\approx 20^\circ \times 10^\circ$. Pixels are integrated with commercial satellite television LNBF (LNB with feedhorn), and the down-converted RF signal is passed into a logarithmic power detector.

The 53 analog channels are organized in groups of 8 in rack-mount electronics enclosures, where the output signal of the power detector is digitized by a 20 MHz 14-bit FADC on a VME board developed by the Electronics Design Group at the Enrico Fermi Institute at University of Chicago. An on-board FPGA is used for digital signal processing and trigger.

The MIDAS trigger, implemented in the FPGAs of the FADC boards, selects candidate events by pixel topology

and time coincidence requirements. For each pixel, the signal is continuously digitized and the running ADC sum of 10 consecutive time bins is calculated. Whenever this sum falls below a preset threshold, a First Level Trigger (FLT) is issued for the pixel and a $10 \mu\text{s}$ gate is opened. This threshold is adjusted every second to keep the FLT rate close to 100 Hz. The Second Level Trigger (SLT) performs a search for pre-defined patterns of FLT triggers whose gates overlap in time. Valid patterns correspond to the expected topology of a cosmic ray shower (straight tracks across the camera). When a SLT is issued, a stream of $100 \mu\text{s}$ of ADC data (including 500 pre-trigger samples) is stored in memory for each of the 53 channels.

Several sources of GHz RF interference were observed to be present in the urban environment of the University of Chicago campus, including cellular phone towers, various motors, and most notably the navigation system of airplanes overflying the MIDAS antenna on their route to Midway Airport. The RF interference may increase suddenly, generating bursts of events during several seconds. Similar interference was observed at the AMBER installation at University of Hawaii. Significant improvement of the background conditions were observed with the installation of bandpass filters designed specifically to cut out the airplane transmission frequency.

Calibration of the MIDAS prototype was performed both during its commissioning and periodically during data taking. A relative calibration is performed using a log-periodic antenna positioned at the center of the reflector, excited by an RF pulse generator. The antenna illuminates the whole camera with a 4 GHz RF pulse of a few μs pulse width, with pulse power varied from -60 to 0 dBm in 5 dBm steps. The antenna will be used to monitor the stability of the system during data taking by firing a set of 10 pulses with fixed power and duration every 15 minutes.

An absolute calibration of MIDAS was performed using several astronomical sources, including the Sun, the Moon ($\approx 0.01 F_{\odot}$), and the Crab Nebula ($\approx 10^{-3} F_{\odot}$), giving an effective system temperature of $\approx 120 \text{ K}$.

Based on the measurements from Gorham et al. [1], using quadratic energy scaling and the measured system temperature, a MIDAS pixel viewing the shower maximum of a 5 EeV shower at 10 km distance would measure ≈ 2000 ADC counts under the baseline. With linear scaling, a 10 EeV shower at the same distance would yield ≈ 200 ADC counts, as compared to the measured pixel baseline fluctuation of about 70 ADC counts. Thus, the MIDAS prototype has a good sensitivity for UHECR detection.

In addition, an end-to-end Monte Carlo simulation of the MIDAS prototype was developed, including the camera beam patterns and the absolute calibration, which is being used for a realistic estimate of the event rate, and for the characterization of the expected events in the same format as the data. An example of a simulated event is shown in Fig. 4.

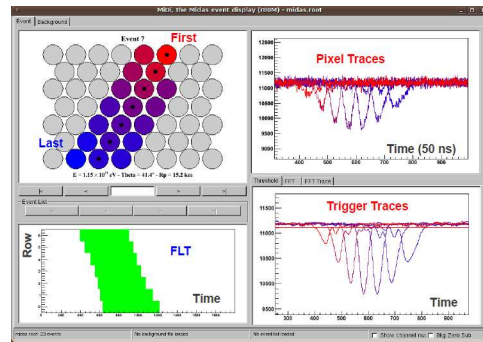


Figure 4: Event display of a simulated MIDAS event. Top left: FLT pixels with color indicating increasing trigger time from light (red) to dark (blue). Top right: FADC traces for selected pixels. Bottom left: FLT trigger gate integrated over all pixels in a row versus time. Bottom right: ADC running sum for selected pixels.

The MIDAS prototype has been in stable operation for 6 months at the University of Chicago, and is in the process of being relocated to the Los Leones FD site.

4 FDWave

The aim of the FDWave project is to develop a microwave telescope equipped with a matrix of radio receivers taking advantage of the existing infrastructure in the Pierre Auger Observatory. The integration of microwave detectors in the Auger Observatory will be performed by installing GHz antennas in installed pixels without photomultipliers (PMTs) at the Los Leones FD site (264 total). The firmware of the FD trigger boards will be modified in order to exclude the microwave signal from the trigger decision. In coincidence of a shower detected by the FD telescopes, the microwave signal will be acquired and registered in the standard data format used by the Auger Collaboration. Extrapolating the reconstructed longitudinal profile within the FOV of the antennas and comparing the energy deposit with the microwave signal, it will be possible to obtain important information on the emission yield and then on the feasibility of this new detection technique.

A careful study of the FD optics [5] and of its use at the GHz frequencies has been performed. The spherical mirrors (3.4 m curvature radius) of Los Leones are of the aluminum kind and therefore conveniently reflecting. The spherical focal surface has a radius of 1.743 m and the detectors are placed in the holes of an aluminium camera body. The camera geometry puts a constraint on the lowest detectable frequency - feeds below 9 GHz are too big and cannot be used with the present camera geometry. This minimum frequency is very close to the Ku-band. Staying within this band has the important advantage of the low cost of the instrumentation due to their large commercial diffusion. The optimal radio receiver fitting the camera geom-

etry constraints is the "RED Classic" straight-feed 40 mm LNB manufactured by Inverto.

The simulation of the FD optics including the diaphragm aperture and camera shadow shows that at 11 GHz, the pixel field of view is $\sim 0.7^\circ$. The telescope gain is ~ 44 dBi and the dish effective area is ~ 1.35 m². With those parameters the telescope should provide evidence of the microwave emission for showers above 3 EeV with quadratic signal scaling. The sensitivity can be significantly improved averaging the FADC traces over many shower profiles, an operation that can be successfully and easily performed using the shower parameters reconstructed by the FD photomultipliers.

5 EASIER

The aim of the EASIER project is to observe radio emission in both the GHz and MHz regime from air showers by antennas installed on each water Cherenkov tank of the SD. Each microwave antenna covers a large field of view of $\approx 60^\circ$ angle around zenith. The RF signal from the antenna is fed into a logarithmic power detector, and then digitized at 40 MHz using the existing SD electronics. In addition, EASIER will benefit from the existing power distribution and communication at the SD station, which greatly simplifies its integration into SD data taking. Since the signal of the EASIER antenna is digitized by the same FADC as the PMTs at each SD station, timing is automatically provided and EASIER data are saved whenever an SD station triggers. As with AMBER and FDWave, the external triggering approach imposes no requirements on the signal to noise ratio of the radio emission, which, under realistic noise conditions, gives a gain of a factor of 3 to 5 relative to self-triggering.

While the effective area of the EASIER antennas is much smaller than the other detectors, the antennas will be significantly closer to the shower axis and within ≈ 3 km from shower maximum, as opposed to ≈ 10 km for dish-type antennas. In addition, due to the short distance from the shower axis, the radio signal is compressed in time typically by a factor of 10. In principle, these factors will compensate for the smaller effective area of the EASIER antenna.

EASIER prototype antennas have been installed in two hexagons of SD stations, one with GHz antennas (seen in Fig. 5) and one with MHz antennas. The MHz detectors consist of a fat active dipole antenna (as used in CODALEMA [4]) with a 36 dB LNA, with additional filters restricting the frequency range to 30 – 70 MHz. The GHz detectors consist of a DMX241 LNB feed, at the top of a 3 m mast looking vertically, and passed through a power detector. The signals are then adapted to the SD FADC input range, resulting in a measurement range of -20 to +30 dB relative to background for the MHz detector, and -20 to +20 dB relative to background for the GHz de-



Figure 5: One of 7 Auger SD stations with a GHz EASIER antenna (right mast).

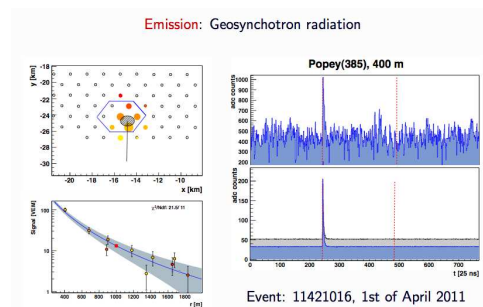


Figure 6: Event display of a cosmic ray seen in the SD and in an EASIER MHz antenna. The hexagon in the top left indicates the tanks with EASIER MHz antennas. Signals in the MHz antenna and SD station are visible in the top and bottom right, respectively.

tor. An event seen by the SD and EASIER MHz antennas is shown in Fig. 6.

6 Conclusion

Multiple detector prototypes are currently under construction at the Pierre Auger Observatory to attempt to observe microwave emission from cosmic ray showers. Using the unique resources of the world's largest cosmic ray observatory, data regarding the microwave emission from UHE-CRs will soon determine whether or not this detection technique is viable.

References

- [1] P. Gorham *et al.*, *Phys. Rev. D*, 2008, **78**: 032007.
- [2] Naval Air Warfare Center: 1999, *Electronic warfare and radar systems engineering handbook*.
- [3] T.H.-J. Mathes for the Pierre Auger Collaboration, paper 0761, these proceedings.
- [4] D. Ardouin *et al.*, *Nucl. Instr. Meth. A*, 2007, **572**: 481-482.
- [5] J. Abraham *et al.*, *Nucl. Instr. Meth. A*, 2010, **620**: 227-251.

Acknowledgments

The successful installation, commissioning and operation of the Pierre Auger Observatory would not have been possible without the strong commitment and effort from the technical and administrative staff in Malargüe.

We are very grateful to the following agencies and organizations for financial support:

Comisión Nacional de Energía Atómica, Fundación Antorchas, Gobierno De La Provincia de Mendoza, Municipalidad de Malargüe, NDM Holdings and Valle Las Leñas, in gratitude for their continuing cooperation over land access, Argentina; the Australian Research Council; Conselho Nacional de Desenvolvimento Científico e Tecnológico (CNPq), Financiadora de Estudos e Projetos (FINEP), Fundação de Amparo à Pesquisa do Estado de Rio de Janeiro (FAPERJ), Fundação de Amparo à Pesquisa do Estado de São Paulo (FAPESP), Ministério de Ciência e Tecnologia (MCT), Brazil; AVCR AV0Z10100502 and AV0Z10100522, GAAV KJB100100904, MSMT-CR LA08016, LC527, 1M06002, and MSM0021620859, Czech Republic; Centre de Calcul IN2P3/CNRS, Centre National de la Recherche Scientifique (CNRS), Conseil Régional Ile-de-France, Département Physique Nucléaire et Corpusculaire (PNC-IN2P3/CNRS), Département Sciences de l'Univers (SDU-INSU/CNRS), France; Bundesministerium für Bildung und Forschung (BMBF), Deutsche Forschungsgemeinschaft (DFG), Finanzministerium Baden-Württemberg, Helmholtz-Gemeinschaft Deutscher Forschungszentren (HGF), Ministerium für Wissenschaft und Forschung, Nordrhein-Westfalen, Ministerium für Wissenschaft, Forschung und Kunst, Baden-Württemberg, Germany; Istituto Nazionale di Fisica Nucleare (INFN), Ministero dell'Istruzione, dell'Università e della Ricerca (MIUR), Italy; Consejo Nacional de Ciencia y Tecnología (CONACYT), Mexico; Ministerie van Onderwijs, Cultuur en Wetenschap, Nederlandse Organisatie voor Wetenschappelijk Onderzoek (NWO), Stichting voor Fundamenteel Onderzoek der Materie (FOM), Netherlands; Ministry of Science and Higher Education, Grant Nos. 1 P03 D 014 30, N202 090 31/0623, and PAP/218/2006, Poland; Fundação para a Ciência e a Tecnologia, Portugal; Ministry for Higher Education, Science, and Technology, Slovenian Research Agency, Slovenia; Comunidad de Madrid, Consejería de Educación de la Comunidad de Castilla La Mancha, FEDER funds, Ministerio de Ciencia e Innovación and Consolider-Ingenio 2010 (CPAN), Xunta de Galicia, Spain; Science and Technology Facilities Council, United Kingdom; Department of Energy, Contract Nos. DE-AC02-07CH11359, DE-FR02-04ER41300, National Science Foundation, Grant No. 0450696, The Grainger Foundation USA; ALFA-EC / HELEN, European Union 6th Framework Program, Grant No. MEIF-CT-2005-025057, European Union 7th Framework Program, Grant No. PIEF-GA-2008-220240, and UNESCO.